

## Article

# Influence of Current Modulation on Melting Behavior during Wire Arc Spraying

Sebastian Weis <sup>1,\*</sup>, Stefan Brumm <sup>1</sup>, Robin Grunert <sup>1</sup>, Jan Morgenschweis <sup>2</sup>, Jürgen Bosler <sup>3</sup> and Thomas Grund <sup>4</sup><sup>1</sup> Westsächsische Hochschule Zwickau, Kornmarkt 1, D-08056 Zwickau, Germany<sup>2</sup> ELMA-Tech GmbH, Wisseraue 1, D-51597 Morsbach, Germany<sup>3</sup> T-Spray GmbH, Hoher Stich 4, D-73525 Lenningen, Germany<sup>4</sup> TU Chemnitz, Straße der Nationen 62, D-09111 Chemnitz, Germany

\* Correspondence: sebastian.weis@fh-zwickau.de; Tel.: +49-375-536-1689

**Abstract:** The atomizing gas dynamics and the applied process energy have a significant influence on the produced particles. The melting process of the two wires can be influenced by current modulation. As for arc welding processes, more and more electronic and software-controlled machines are being used for arc spraying and will have replaced conventional power sources in the future. Due to the highly dynamic, fast regulating computing technology in the latest energy source, technology arcs can be operated with different current forms and types. The modern machines allow process-stable, reproducible variation of the particles and heat input into the substrate. Constant and pulsed current can be used as current forms. Usable current types are direct current (DC) and alternating current (AC). The electrical parameters must be analyzed to evaluate the process behavior. The consumable used is a wire-shaped iron-based alloy with a diameter of 1.6 mm. Relevant process parameters such as basic current  $I_{\text{ground}}$ , pulse current  $I_{\text{pulse}}$ , pulse duration  $t_{\text{pulse}}$ , impulse frequency  $f_{\text{pulse}}$ , and alternating current frequency,  $f_{\text{AC}}$ , are varied and recorded using appropriate measurement technology. The aim is to change the process performance and thereby the particle formation in a broad band. High-speed images are used to observe the arc and the deposition process. In addition, particle sizes are determined.

**Keywords:** wire arc spraying; melting behavior; current modulation; pulsed arc; alternating current; metal powder atomizing; additive manufacturing



**Citation:** Weis, S.; Brumm, S.; Grunert, R.; Morgenschweis, J.; Bosler, J.; Grund, T. Influence of Current Modulation on Melting Behavior during Wire Arc Spraying. *Metals* **2022**, *12*, 1347. <https://doi.org/10.3390/met12081347>

Academic Editor: Hamid Jahed

Received: 29 June 2022

Accepted: 9 August 2022

Published: 13 August 2022

**Publisher's Note:** MDPI stays neutral with regard to jurisdictional claims in published maps and institutional affiliations.



**Copyright:** © 2022 by the authors. Licensee MDPI, Basel, Switzerland. This article is an open access article distributed under the terms and conditions of the Creative Commons Attribution (CC BY) license (<https://creativecommons.org/licenses/by/4.0/>).

## 1. Introduction

Conventional metal powder production on an industrial scale is usually carried out in large-scale plants. In this process, several hundred kilograms are produced per production unit. This is unprofitable for delivering small-volume customers, which use the powders for prototype constructions and also for the development of new alloys for laser additive manufacturing. Wire arc spraying could be an alternative process for the production of metal powders. This is an inexpensive coating process with low thermal stress on the substrate and a low degree of dilution. Aluminum, copper, iron, nickel, and their alloys can be processed. Spraying with two different materials to form an alloy or pseudo-alloy is also possible [1].

The atomizing gas dynamics and the applied process energy have a significant influence on the produced particles. High velocity arc spraying (Laval system) was derived from the original process [2–4]. The melting process of the two wires can be influenced by current modulation using electronic and software-controlled machines as in arc welding processes [5]. Regarding the modification of the atomizing gas dynamics, the atomization is refined with improved nozzle geometry or higher gas pressures and speeds. As a result, denser layers with a low oxide content and improved adhesive strength are formed [6–9]. On average, smaller spray particles are observed as the atomizing gas flow

rate increases [10]. The investigation indicates that smaller particles have two direct influences on the coating result due to the flight phase. On the one hand, smaller particles showed a significantly higher degree of oxidation in the process with air as the atomizing gas. On the other hand, they cooled down faster in the spray jet than the larger fraction. The reason for this is the specific surface of the spray particles. The heat dissipation in the process essentially takes place via thermal radiation. The relation of the small volume to the large surface favors this behavior. The reactions with the surrounding medium also take place on the surface. The smaller the particle, the greater the relation of surface area to internal volume and the faster it can oxidize [10].

The disadvantage compared to other thermal coating processes is the inhomogeneity and porosity of the produced layer. It is known from the literature that in wire arc spraying with constant DC, the cathode and anode have different melting rates and particle formation behavior. With the same feed speed of both wires, the arc moves out of the center of the gas flow. On the side of the cathode the material melts faster. The particles that were primarily torn off are obviously larger than those of the opposite wire tip [11]. In experiments by Pourmousa et al., it has been shown that the particles on the cathode side are, on average, only half the size of the particles on the anode side [12]. Liao et al. also describe different particle size distributions of both electrodes in their publication [13].

According to Hussary et al., the formation of the particles in the constant DC process from the melt is divided into three phases [14,15]. First, the wire melts and drops form on the wire tips. The melt can detach from the wire tips axially, not axially symmetrically to the atomizing gas flow (preferably on the anode side) or as a metal vapor (mainly on the cathode side). When the arc is reaching the end of the wires, the power of the arc tears the melt off. The change in the arc within the constant DC process is reflected in the electrical voltage. The second phase is the primary atomization. The critical volume of melt is generated and the viscous droplets form thread-like melt structures at the electrode tips. This happens due to the heat input and in interaction with the atomizing gas behavior. In the last phase, the melt will be further atomized. The primary formed melt and droplets are geometrically not stable in type and size. In the end area of the wires, the atomizing gas is highly turbulent. Therefore, differences in pressure occur, which tear the melt and droplets into small pieces, accelerate, and form them into spherical particles.

For wire arc spraying with pulsed DC and AC, the following advantages can be expected: The uniform melting of the two wires can increase the deposition rate, reduces the thermal treatment of the substrate, and produces homogeneous layers with less porosity. For the pulsed DC process, a reduction in particle size was determined in [16,17]. The effect of targeted droplet detachment of the molten filler material, known from the gas metal arc welding (GMAW) as pulsed arc, is also described in the literature as a possibility for improving particle distribution in wire arc spraying. The pinch effect at the GMAW makes it possible to form one droplet per current impulse. A low base current  $I_{\text{ground}}$  is set. The full melting power is frequently generated by a pulsed voltage signal  $U_{\text{pulse}}$ , which leads to an increase from the base current to the pulsed current  $I_{\text{pulse}}$ . The background to the application of this method is the targeted detachment of a specific mass of melt per current pulse using the pinch effect. The reason for the radial constriction of the liquid or viscous melt is a magnetic field vertical to the arc axis, the Lorentz force. The strength of this magnetic field is directly dependent on the current flow and the surrounding medium. A pulsed strong increase in the current flow causes the magnetic field to suddenly increase and the resulting constriction force to increase. This phenomenon favors droplet detachment. The arc characteristics during wire arc spraying are directly linked to the current/voltage behavior of the system. As a result of the continuous melting and tearing off of the melt at the wire ends, the arc constantly varies in intensity and length. In addition, the generated arc migrates with the melt in direction of the spray jet due to the force of the atomizing gas pressure. If the melt is dissolved, the process begins again. The recording superimpositions of the voltage curve with synchronized high-speed recordings proves that the frequency and the amplitudes correlate with the fluctuating arc behavior [18,19]. The use of pulsed

AC reduces the heat input into the component during welding [20–22], which can lead to a reduction in the thermal load on the substrate during wire arc spraying. Furthermore, metallurgical influences are also exerted on the solidification of the coating material, the resulting microstructure, and the adhesion of the coating to the substrate. To be able to use the pulsed DC and AC processes when coating materials, an appropriate energy source is necessary to implement the process. The hardware components and control technology of the machine must meet the requirements. The use of pulsed voltage sources in wire arc spraying, called Pulsed Wire Arc Spray (PWAS), was already discussed in 1988 [23] and was first examined and described in 2005 [24]. In the present work, the influence of current modulation on the melting behavior in wire arc spraying is investigated. Non-pulsed wire arc spraying processes have a high fraction range due to the stochastic particle detachment on the wire and the differences between the anode and cathode side. With the help of pulsed processes, the detaching particle size can be influenced and ultimately a narrower particle fraction can be achieved. Processes such as laser additive manufacturing that use the produced powders can only use a close fraction of powder size. The main problem is the large number of parameters that influence pulsed processes, for example: basic current  $I_{\text{ground}}$ , pulse current  $I_{\text{pulse}}$ , pulse duration  $t_{\text{pulse}}$ , impulse frequency  $f_{\text{pulse}}$ , alternating current frequency  $f_{\text{AC}}$ . The aim is to specifically control the melting behavior to produce targeted particle sizes.

## 2. Materials and Methods

A wire-shaped iron-based alloy material number 1.5130 (mas-%: C 0.1–0.13, Mn 1.6–1.8, Si 0.25–0.4, Cr  $\leq$  0.1, Ni  $\leq$  0.1, Cu  $\leq$  0.1, Mo  $\leq$  0.05) with a diameter of 1.6 mm and nitrogen (N) as the atomizing gas is used for the investigations. High-speed recordings and current/voltage curves are recorded for analysis. A high-speed camera (FASTCAM Mini AX200, VKT GmbH, Pfullingen, Germany), filter and exposure laser (Cavilux, Cavitar Ltd., Tampere, Finland) and a real-time measurement system from National Instruments (cRIO-9067, National Instruments Corporation, Austin, TX, USA) are used for this purpose (Figure 1). The current is tapped in series and the voltage is located close to the arc directly at the current contact tips. A new energy source from ELMA-Tech (ELMA-Tech GmbH, Morsbach, Germany) is used, which can implement constant DC, pulsed DC, and pulsed AC. The torch technology comes from T-Spray GmbH (Lenningen, Germany). The used closed nozzle system has the advantage that the perforated aperture bundles the spray jet, generates additional turbulence around the ends of the wire and thus improves the evaporation of the melt. The wire drive is an electric motor in a push–pull design and ensures a smooth wire feed. Due to the multitude of adjustable process parameters, which in turn depend on each other, several challenges have to be solved for the pulsed processes.

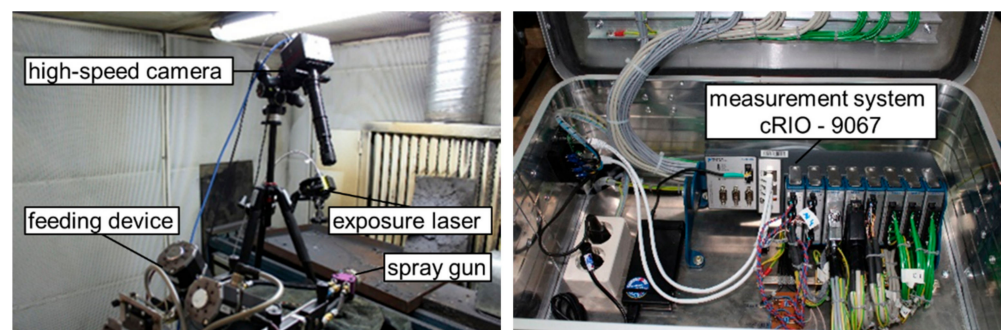


**Figure 1.** Experimental setup for determining particle detachment, (left): high-speed camera, (right): NI cRIO measurement system.

In tests wire feed speeds between 3 to 12 m·min<sup>−1</sup> are investigated. The arc voltage is varied for the constant DC process. For the pulsed processes, the pulse frequencies as well as the ground current and pulse current height have to be coordinated with each other.

With the help of a developed particle trap, the spray particles are collected in a container (Figure 2). The spray gun (T-Spray GmbH, Lenningen, Germany) is mounted vertically over a spray chamber. Thus, gravity in combination with the 2 m long spray chamber supports a cooling of the molten particles. Nitrogen is used as the atomizer gas to reduce particle oxidation. Through a cone, the particles reach the cyclone in a pipe system. An incoming transport gas at the beginning of the pipeline has the function of particle cooling, protection against oxidation, and support of the particle movement towards cyclone. The cyclone, in combination with extraction, results in separation of particle and removal of hot gas.

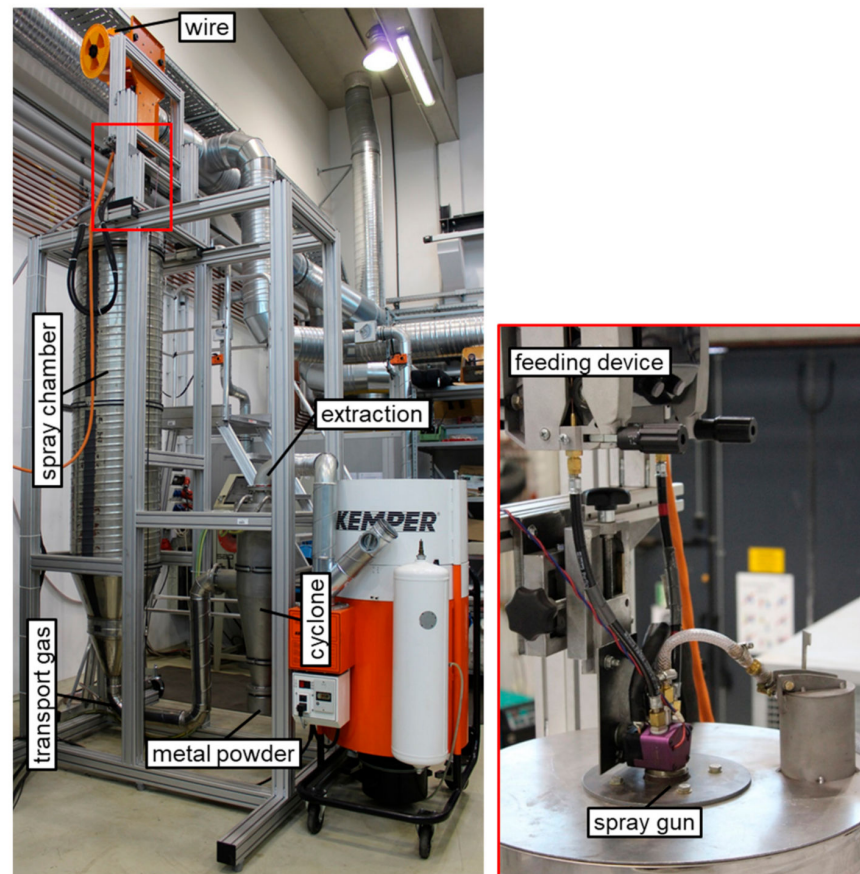


**Figure 2.** Experimental setup for the production of metal powders.

The entire system is supported and mounted in aluminum profiles.

From the three groups of separation, sedimentation, and counting methods for determining the particle size, the sieve analysis is selected from the separation methods. The evaluation of the sieve analysis is performed according to [25] as follows:

- the “class” is the interval between the individual mesh sizes of the upper and lower limiting test sieve
- the “ $\Delta D$  fraction” is the powder mass belonging to a particular class
- the “passage D” is the sum of the fractions that have passed the corresponding sieve
- the “residue R” is the sum of all fractions remaining on the sieve

### 3. Results

#### 3.1. Influence of Current Form and Type on Arc and Particle Formation

##### 3.1.1. Direct Current

Particle formation and detachment during wire arc spraying with direct current is described by Hussary. The arc moves continuously back and forth at the melted wire ends. In Figure 3 on the left, the arc is close to the current contact nozzle. At this moment, the arc



voltage is low. The melt between the wires is pushed out by the atomizer gas pressure. In Figure 3 on the right, the arc moves towards the end of the wire. The arc length and thus the arc voltage increases. In Figure 4 on the left, 50  $\mu$ s later, the arc length is approximately the same. The quantity of the melt increases. On the anode side (electrode at the bottom), the melt forms a filament. On the cathode side, melt is torn off like drops. In Figure 4 on the right, the arc moves back to the point of the shortest distance towards the current contact nozzle. The arc length and the current decrease. To prevent a cut-off of the arc, the spraying machine regulates the current up and the process is starting again. More material is melted on the cathode side. This can be seen from the different lengths of the wire ends.

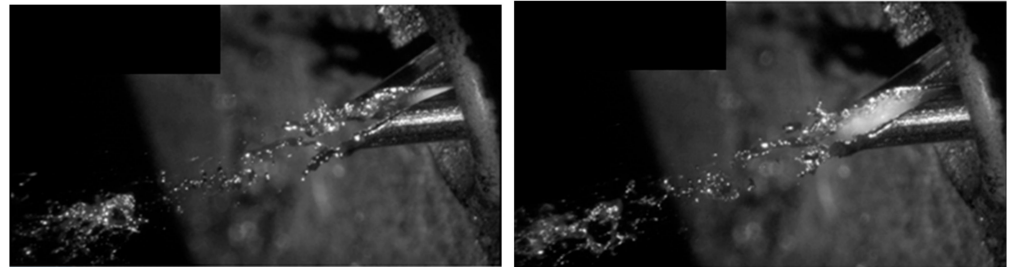


**Figure 3.** Particle formation during wire arc spraying with direct current at time (left):  $t = 35.85$  ms, (right):  $t = 35.90$  ms.

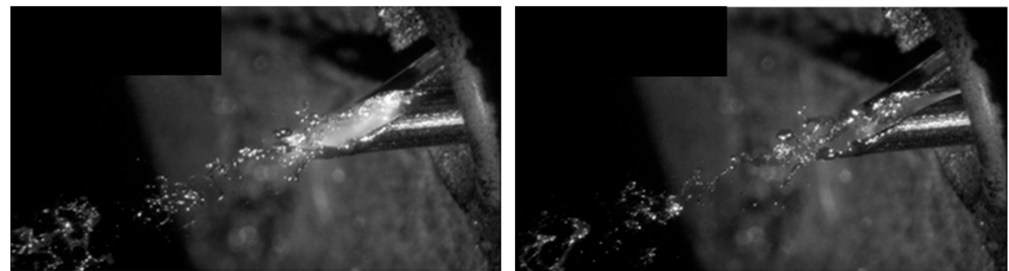


**Figure 4.** Particle formation during wire arc spraying with direct current at time (left):  $t = 35.95$  ms, (right):  $t = 36.00$  ms.

In all pictures of Figures 3 and 4, it can be seen that the melt is not directly atomized into small drops at the wire ends, but only at a distance of about 7.5 mm (cf. Introduction).

### 3.1.2. Pulsed Direct Current

After the pulse current phase, the arc moves towards the contact nozzle. In Figure 5 on the left, the process is in the base current phase. The arc length and current are low. The process heat is directly related to the spray power. This is calculated from the product of current and voltage. Therefore, the process heat is low at time  $t = 11.4$  ms. As a result, only a few molten drops detach from the wire ends and only a small amount of melt is accelerated towards the substrate. In the pulse current phase (Figure 6, left), the point-shaped starting point of the arc at the cathode (upper electrode) is clearly visible.

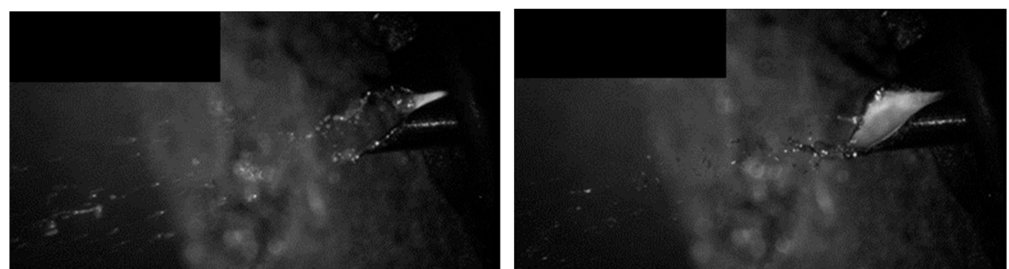


**Figure 5.** Particle formation during wire arc spraying with pulsed direct current at time (left):  $t = 11.4$  ms, (right):  $t = 12.2$  ms.

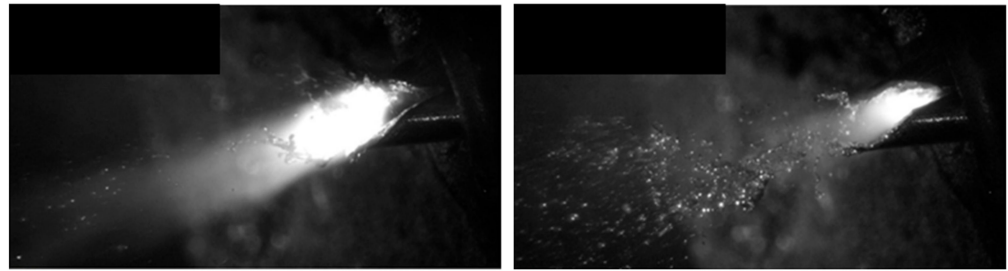


**Figure 6.** Particle formation during wire arc spraying with pulsed direct current at time (**left**):  $t = 12.6$  ms, (**right**):  $t = 13.0$  ms.

The current and the process heat increase sharply. A small amount of melt detaches from the cathode during the pulse current phase. Afterwards (Figure 6, right), the arc moves in the direction of the current contact nozzle due to the reduction of the current. This happens in the same way in the direct current process. The melt generated in the pulsed current phase is accelerated towards the substrate in form of droplets. In contrast to wire arc spraying with direct current, the melt produced at the wire ends is directly divided into finer droplets by the force of the arc in the pulsed current phase.

### 3.1.3. Pulsed Alternating Current

After the pulse current phase, the arc moves towards the contact nozzle (Figure 7, left). At this time ( $t = 192.8$  ms), the process is in the base current phase and shows the same process behavior as the pulsed DC process. In Figure 7 on the right, the process is still in the base current phase. The arc is blown towards the end of the wire by the atomizing gas pressure. The polarity has changed. In the pulsed current phase (Figure 8, left), the arc length and current intensity increase abruptly.

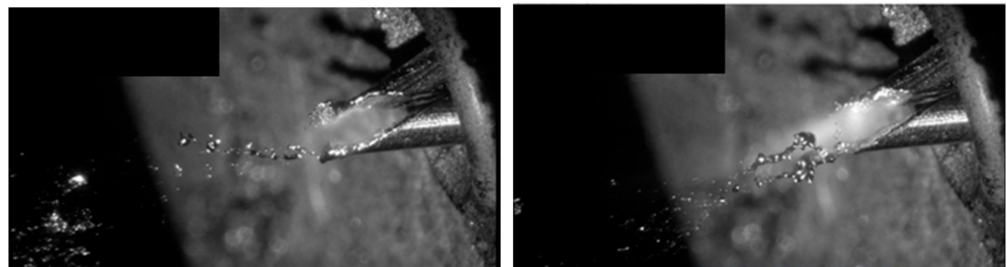


**Figure 7.** Particle formation during wire arc spraying with pulsed alternating current at time (**left**):  $t = 192.8$  ms, (**right**):  $t = 193.4$  ms.

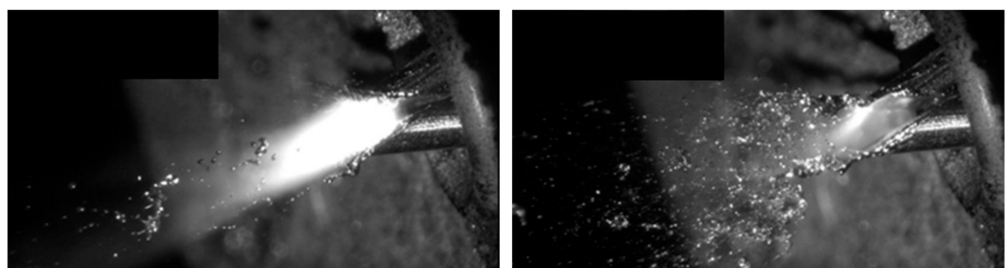


**Figure 8.** Particle formation during wire arc spraying with pulsed alternating current at time (**left**):  $t = 194.0$  ms, (**right**):  $t = 194.35$  ms.

At the wire ends, the melt is blown off. The distance between the two electrodes increases. After that, the process goes into the base current phase (Figure 8, right). The process heat is reduced. The previously formed melt is accelerated towards the substrate in the base current phase. Here, as in the pulsed direct current process, finer droplets are

produced directly after the pulse current phase. It is noticeable that the two wire ends show a uniform melting behavior.

### 3.2. Influence of the Process Parameters on the Spray Power

#### 3.2.1. Direct Current

In wire arc spraying with direct current, the spray power can be varied by the wire feed speed. Within a wire feed speed, the spray power can also be changed by the specified voltage. Figure 9 shows the arc voltage of 25, 30, and 35 V for a wire feed of  $6 \text{ m}\cdot\text{min}^{-1}$  as a function of the spray power.

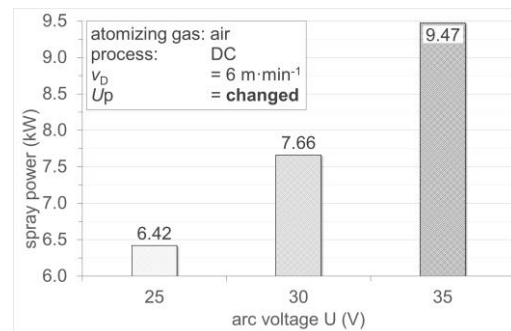


**Figure 9.** Comparison of the spray power as a function of the arc voltage with direct current.

It can be seen that the used wire can be processed reliably at a wire feed speed of  $6 \text{ m}\cdot\text{min}^{-1}$  and a spray power between 6.4 and 9.5 kW. When comparing the current/voltage curves with direct current of 25 and 35 V (Figure 10), it is noticeable that at higher voltages the current increases and decreases periodically. This course can be traced back to the “back and forth” movement of the arc described under Section 3.1.1 and to the  $\Delta I$  control (constant voltage) of the machine. When the voltage is set low, the fluctuation of the current intensity is discontinuous. The set voltage of 25 V fluctuates between about 15 and 35 V and corresponds on average (24 V) approximately to the specified value. By increasing the set voltage to 35 V, the real voltage fluctuates between about 17 and 45 V and also corresponds on average (34 V) to the set value. The difference of 1 V results from the different measuring points of the voltage. On the machine side, the voltage is tapped internally. Therefore, the voltage drops in the power lines are not considered.

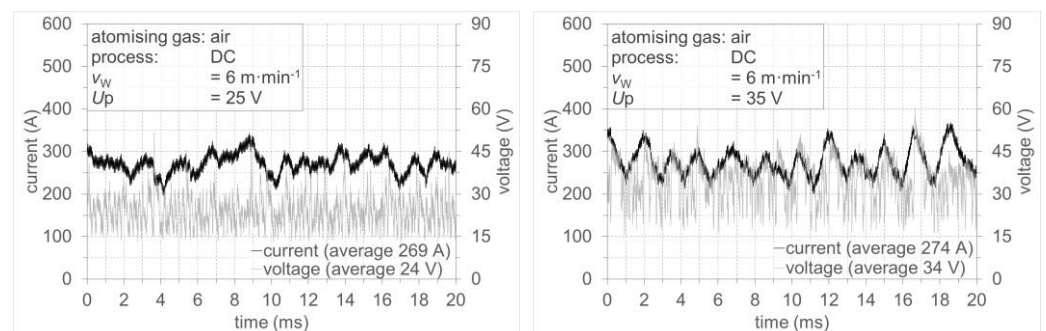


**Figure 10.** Current/voltage curve, direct current, (left):  $U = 25 \text{ V}$ , (right):  $U = 35 \text{ V}$ .

#### 3.2.2. Pulsed Direct Current

With pulsed direct current, the spray power can be varied by different process parameters within a wire feed speed. These are, on the one hand, the level of the pulse current via the pulse voltage  $U_p$ , and on the other hand, the base current  $I_{\text{ground}}$ . In addition, the spray power can be changed via the pulse frequency. The major influence is achieved by the pulse current level ( $\Delta P = 2 \text{ kW}$ ). Figure 11 shows the influence of the pulse voltage on the left and the base current on the right. The pulse frequency can be used to set the spray power at a wire feed of  $6 \text{ m}\cdot\text{min}^{-1}$  from 7.3 up to 8.3 kW (Figure 12). Figure 13 compares the

current/voltage curves of pulsed direct current with different pulse voltages. It can be seen that increasing the pulse voltage from 45 to 55 V leads to an increase in the pulse current level from about 425 to about 475 A. Furthermore, it can be observed that at  $U_P = 45$  V the voltage fluctuates constantly between 15 V and about 35 V. At  $U_P = 55$  V, the voltage rises to about 50 V shortly after the pulse current.

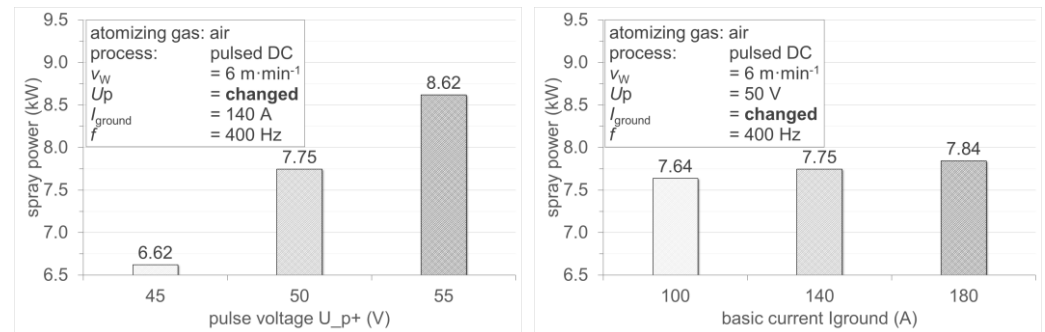


**Figure 11.** Comparison of the spray power as a function of the pulse voltage (left) and the base current (right) with pulsed direct current.

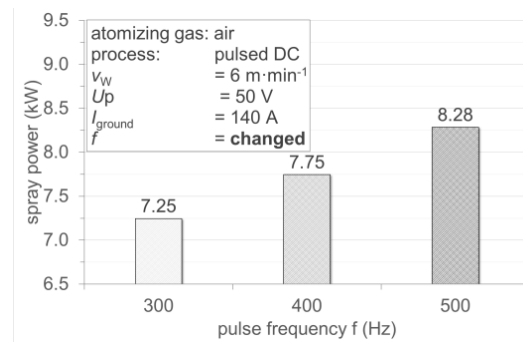


**Figure 12.** Comparison of the spray power as a function of the pulse frequency with pulsed direct current.

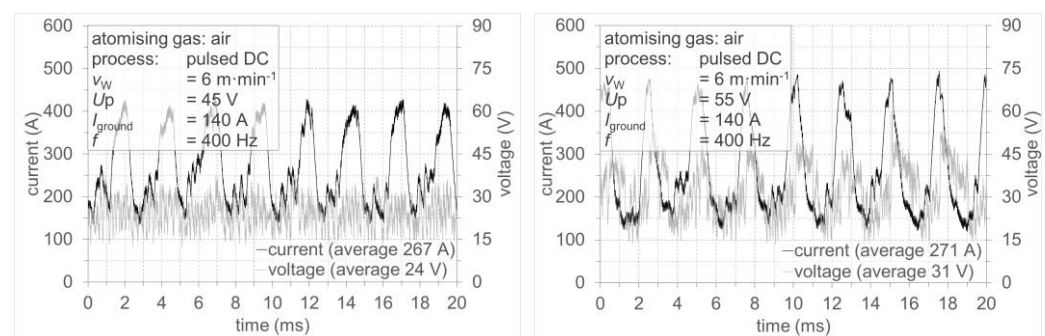


**Figure 13.** Current/voltage curve, pulsed direct current, (left):  $U_P = 45$  V, (right):  $U_P = 55$  V.

The reason for this is the high heat input. A larger amount of molten material is released from the wire ends compared to the lower pulse current. This increases the distance between the wires, which leads to an increase in the arc voltage. This is also shown by the average arc voltage, which increases from 24 V to 31 V. It is interesting to note that the average current only increases slightly. The higher energy input by increasing the pulse frequency from 300 to 500 Hz (Figure 14) leads to an extension of the arc length. The average voltage increases from 27 to 30 V and the average current remains at the same level.



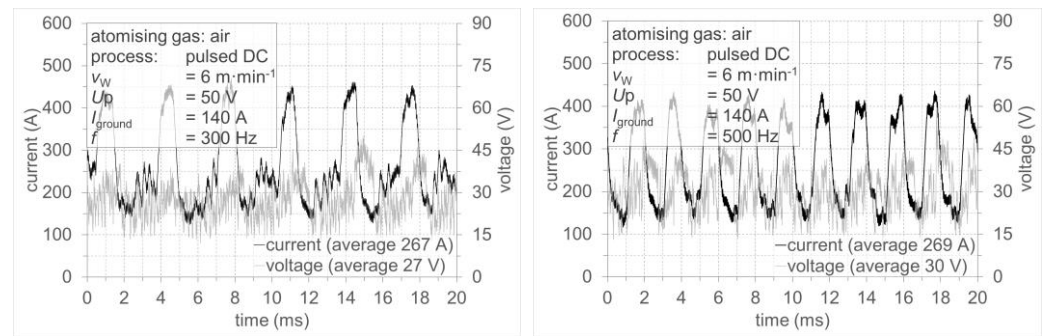


**Figure 14.** Current/voltage curve, pulsed direct current, (left):  $f = 300 \text{ Hz}$ , (right):  $f = 500 \text{ Hz}$ .

### 3.2.3. Pulsed Alternating Current

With pulsed alternating current, the spray power can also be varied by the pulse and the basic current level. Figure 15 shows the influence of the two parameters on spray power. With the pulsed alternating current process, the spray power can be varied between 6.2 and 7.5 kW at a wire feed rate of  $6 \text{ m}\cdot\text{min}^{-1}$ .

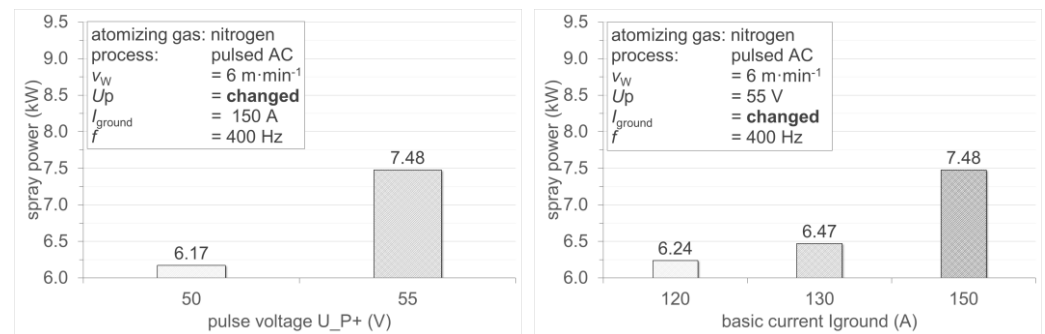


**Figure 15.** Comparison of the spray power as a function of the pulse voltage (left) and the base current (right) with pulsed alternating current.

Changing the pulse voltage from 50 to 55 V causes the pulse current level to rise from about 425 to 450 A (Figure 16). Furthermore, the average voltage and the average current increase. As a result, the spray power increases by 1.3 kW.

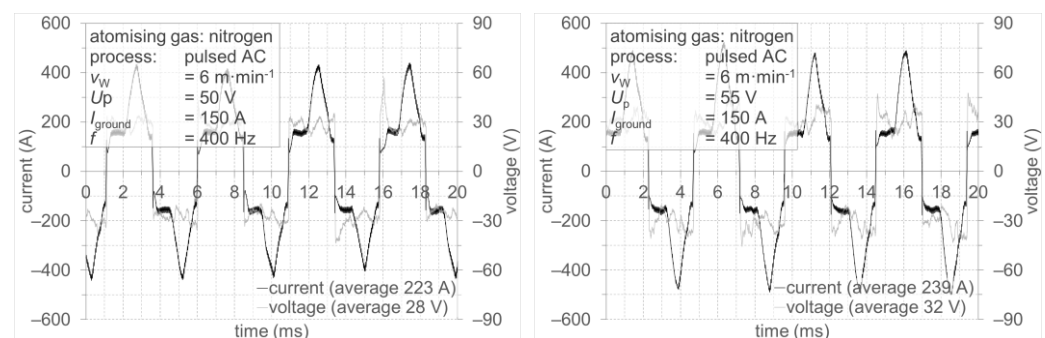


**Figure 16.** Current/voltage curve, pulsed alternating current, (left):  $U_p = 50 \text{ V}$ , (right):  $U_p = 55 \text{ V}$ .

When the base current level is changed from 120 to 150 A, pulsed alternating current ( $\Delta P = 1.3 \text{ kW}$ ) exerts a bigger influence on the spray power than pulsed direct current ( $\Delta P = 0.2 \text{ kW}$ ). Figure 17 shows the current/voltage curves with different base currents. The average current, as well as the average voltage of the process, changes.

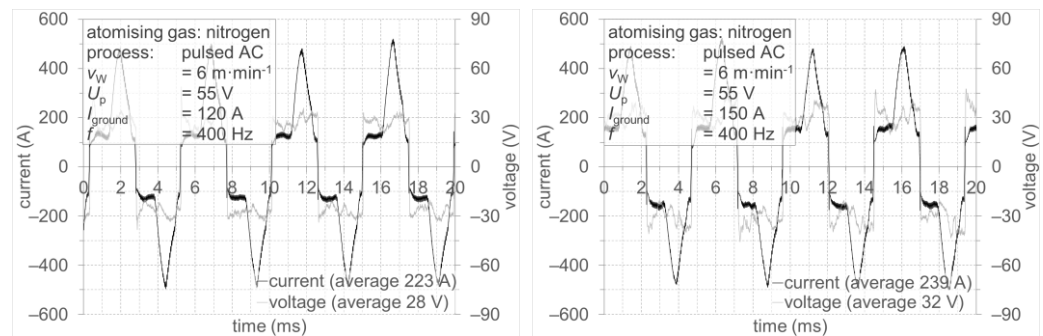


**Figure 17.** Current/voltage curve, pulsed alternating current, (left):  $I_{\text{ground}} = 120 \text{ A}$ , (right):  $I_{\text{ground}} = 150 \text{ A}$ .

### 3.3. Particle Analysis

The first batches of metal powder were produced using the particle trap shown in Figure 2. Nitrogen was used as the atomizing gas. For this purpose, the parameter wire feed speed was varied and the influence of the current form (direct current and pulsed direct current) on the particles was investigated. Figure 18 shows the distribution of the grain classes as a function of the current form and the wire feed speed. It can be seen that most of the particles are in the class between 50 and 150  $\mu\text{m}$ . A significant difference of the classes depending on the current form and the wire feed speed cannot be determined.

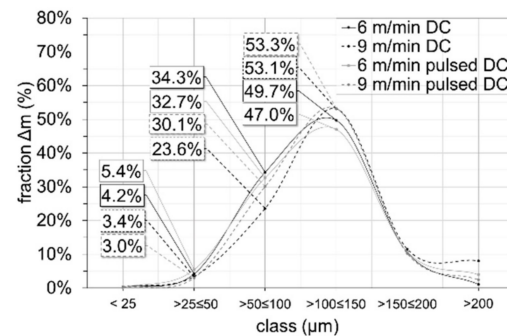


**Figure 18.** Distribution of the classes as a function of the current form and the wire feed speed.

A closer look at the metal powder exemplarily produced with pulsed direct current and a wire feed speed of  $6 \text{ m}\cdot\text{min}^{-1}$  shows that the majority of the particles have a spherical shape with a diameter of 50 to 150  $\mu\text{m}$ . Furthermore, there are other components with an irregular shape in the powder, which are bar-shaped, for example. In terms of dimensions, these deviate significantly from the desired spherical shape and have a length of up to 550  $\mu\text{m}$  (Figure 19). The measurement of the element distribution (Figure 20) was shown as an example for a point measurement. Several measurements were carried out and all had the same result. When looking at Figure 20, all particles are clearly covered by an oxide layer. This layer is about 20  $\mu\text{m}$  thick and consists mainly of iron oxide. In the shell surface area, the percentage mass distribution of the elements shows an oxygen content of 28%. After evaluating the results, it was found out that there is a leak in the atomization system. Atmospheric oxygen enters the process chamber, and as a result, the particles oxidize. This happens at the point where the batch cooling takes place. We are currently working on a modification of the system to avoid this oxidation. The oxidation initially makes the particles unusable for subsequent processes. However, this does not affect the investigation of the influence of the electrical parameters on particle detachment, which is the main subject of this work. Another striking feature is the manganese distribution in comparison of particle core and particle shell. Compared to the chemical composition of the material (see Section 2), there is too little manganese in the core (0.3%) and far too much in the coating (6%). One possible explanation is that the majority is present as manganese dioxide in the particle shell, and therefore only a small amount exists in the core.

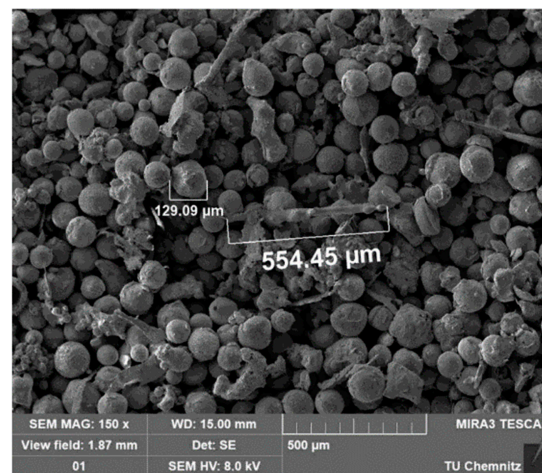


Figure 19. Particle structure and dimensions of metal powder ( $v_w = 6 \text{ m} \cdot \text{min}^{-1}$ , pulsed direct current).

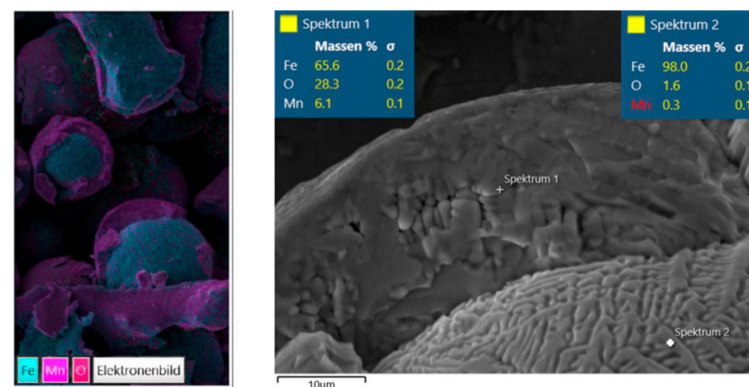


Figure 20. Element distribution in the particles.

#### 4. Conclusions

The paper presents the research work on an alternative type of metal powder production for laser additive manufacturing. Wire arc spraying can be used to produce powders from wire material. For this purpose, a spray gun is mounted vertically above a spray chamber. In the spray chamber, the particles cool down and a shielding gas is used to prevent oxidation. The solidified particles pass through a pipe system into the cyclone and finally fall into the particle trap.

The focus of the investigation is to control the melting behavior by means of current modulation. Different current types were reported, and their possibilities and limitations were analyzed using high-speed recordings and current/voltage curves. A variation of the spray power is possible with direct current, pulsed direct, and alternating current. Spraying with direct current, only the set arc voltage has an influence on the melting behavior. For pulsed processes, these are the base current, the pulse current, and the pulse frequency.

Finally, the open questions and biggest challenges related to powder production are discussed in order to point out directions for future research. The particle analysis has shown that the used particle trap draws secondary air. This is evident from the oxide content of the particles. The produced powders are processed in subsequent production steps, e.g., by plasma powder build-up welding. For this purpose, it is necessary to eliminate the secondary air and the resulting oxide content on the particles.

To determine which current modulation has the biggest impact on the produced powder, further investigations must be carried out. For this purpose, more powder samples are produced, and the parameters for the pulsed alternating current process are varied. In addition, the used wire materials are expanded, for example, 316L.

**Author Contributions:** Conceptualization, S.W.; investigation, S.B.; resources, J.M. and J.B.; data curation, S.B. and R.G.; writing—original draft, S.W., S.B., R.G., J.M., J.B. and T.G.; writing—review & editing, S.W., R.G. and T.G.; visualization, R.G.; supervision, S.W. and S.B.; project administration, S.W.; funding acquisition, S.B. All authors have read and agreed to the published version of the manuscript.

**Funding:** This article was written as part of the “Central Innovation Program” as a cooperative project between the University of Applied Sciences Zwickau, ELMA-Tech GmbH and T-Spray GmbH under the funding code KK5128103KU1 and the title “LDS<sup>3</sup>- wire arc spraying with innovative three-cathode technology and a swirl gas constricted particle jet”.

**Institutional Review Board Statement:** Not applicable.

**Informed Consent Statement:** Not applicable.

**Data Availability Statement:** Data sharing not applicable.

**Acknowledgments:** The research project was funded as part of the Central Innovation Program for SMEs (ZIM) of the Federal Ministry of Economics and Climate Protection (BMWK). We would like to express our heartfelt thanks for this encouragement and support.

**Conflicts of Interest:** The authors declare no conflict of interest.

## References

1. Watanabe, T.; Sato, T.; Nezu, A. Electrode phenomena investigation of wire arc spraying for preparation of Ti-Al intermetallic compounds. *Thin Solid Films* **2022**, *407*, 98–103. [\[CrossRef\]](#)
2. Marantz, D.; Kowalsky, K. High Velocity Electric-Arc Spray Apparatus and Method of Forming Materials. US-Patentschrift US5296667A, 22 March 1994.
3. Carlson, R.; Heberlein, J. Single Wire Arc Spray Apparatus and Methods of Using Same. US-Patentschrift US185473A1, 12 December 2002.
4. Wilden, J.; Schwenk, A.; Bergmann, J.-P.; Zimmermann, S.; Landes, K. Supersonic Nozzles for the Wire Arc Spraying. In Proceedings of the International Thermal Spray Conference, Basel, Switzerland, 2–4 May 2005; pp. 1068–1073.
5. Jäschke, B. *Von Klassischer MSG-Prozessregelung zur Modernen Schweißstromquellenregelung mit “Dynamik“-Verstellung*; Schweißen und Schneiden, DVS Media GmbH: Düsseldorf, Germany, 2014; pp. 600–605.
6. Cooke, K.; Oliver, G.; Buchanan, V.; Palmer, N. Optimisation of the electric wire arc-spraying process for improved wear resistance of sugar mill roller shells. *Surf. Coat. Technol.* **2007**, *202*, 185–188. [\[CrossRef\]](#)
7. Watanabe, T.; Wang, X.; Heberlein, J.; Pfender, E.; Herwig, W. Voltage and Current Fluctuations in Wire Arc Spraying as Indications for Coating Properties. In Proceedings of the Thermal Spray: Practical Solutions for Engineering Problems, Cincinnati, OH, USA, 7–11 October 1996; pp. 577–583.
8. Watanabe, T.; Wang, X.; Pfender, E.; Heberlein, J. Correlations between electrode phenomena and coating properties in wire arc spraying. *Thin Solid Films* **1998**, *316*, 169–173. [\[CrossRef\]](#)
9. Wen, J.; Wen, S.; Zhang, Z.; Geng, W.; Liu, A. (Hg.): Aerodynamic stabilization of the arc in two wire arc spraying. In *Thermal Spraying—Current Status and Future Trends*; High Temperature Society of Japan: Osaka, Japan, 1995; pp. 431–434.
10. Planche, M.; Liao, H.; Coddet, C. Relationships between inflight particle characteristics and coating microstructure with a twin wire arc spray process and different working conditions. *Surf. Coat. Technol.* **2004**, *182*, 215–226. [\[CrossRef\]](#)
11. Zhu, Y.; Liao, H.; Coddet, C.; Xu, B. Characterization via image analysis of crossover trajectories and inhomogeneity in twin wire arc spraying. *Surf. Coat. Technol.* **2003**, *162*, 301–308. [\[CrossRef\]](#)
12. Pourmousa, A.; Mostaghimi, J.; Abedini, A.; Chandra, S. Particle size distribution in a wire-arc spraying system. *J. Therm. Spray Technol.* **2005**, *14*, 502–510. [\[CrossRef\]](#)
13. Liao, H.; Zhu, Y.; Bolot, R.; Coddet, C.; Ma, S. Size distribution of particles from individual wires and the effects of nozzle geometry in twin wire arc spraying. *Surf. Coat. Technol.* **2005**, *200*, 2123–2130. [\[CrossRef\]](#)
14. Hussary, N.; Heberlein, J. Atomization and particle-jet interactions in the wire-arc spraying process. *J. Therm. Spray Technol.* **2001**, *10*, 604–610. [\[CrossRef\]](#)
15. Hussary, N.; Heberlein, J. Primary Breakup of Metal in the Wire Arc Spray Process. In *Thermal Spray—Advancing the Science and Applying the Technology*; ASM International: Materials Park, OH, USA, 2003; pp. 1023–1032.
16. Brumm, S.; Landgrebe, D.; Kunze, S.; Kimme, S.; Weis, S.; Morgenschweis, J. Investigations of A Pulsed DC Arc Spray Process. In Proceedings of the International Thermal Spray Conference and Exposition, Orlando, FL, USA, 7–10 May 2018.
17. Brumm, S.; Landgrebe, D.; Kunze, S.; Kimme, S.; Weis, S.; Morgenschweis, J. *Lichtbogendrahtspritzen mit Gepulstem Gleichstrom: 20*; Werkstofftechnischen Kolloquium: Chemnitz, Germany, 2018.
18. Newbery, A.; Grant, P. Large arc voltage fluctuations and droplet formation in electric arc wire spraying. *Powder Metall.* **2003**, *46*, 229–235. [\[CrossRef\]](#)



19. Hussary, N.; Heberlein, J. Effect of System Parameters on Metal Breakup and Particle Formation in the Wire Arc Spray Process. *J. Therm. Spray Technol.* **2006**, *16*, 140–152. [[CrossRef](#)]
20. Haelsig, A.; Mayr, P. Energy balance study of gas-shielded arc welding processes. *Weld World* **2013**, *57*, 727–734. [[CrossRef](#)]
21. Brumm, S.; Bürkner, G. Gas metal arc pulse welding with alternating current for lightweight materials. In Proceedings of the Conference MEFORM 2015, Light Metals—Forming Technologies and Further Processing, Freiberg, Germany, 25–27 March 2015; Materials Today: Proceedings; Volume 2, pp. 179–287.
22. Brumm, S.; Landgrebe, D. AC-MIG-Puls-Schweißen für Aluminiumlegierungen. In Proceedings of the DVS Congress 2015, Nuremberg, Germany, 14–17 September 2015; DVS Berichte Band 315; DVS Media GmbH: Dusseldorf, Germany, 2015; pp. 254–259, ISBN 978-3-945023-46-4.
23. Steffens, H.; Dvorak, M. Arc and Plasma Spraying today in the 90th. In Surface Modification. In Proceedings of the International Symposium on Strategy of Innovation in Materials Processing—New Challenge for the 21st Century, Osaka, Japan, 17 May 1988.
24. Atzberger, A.; Szulc, M.; Hartz-Behrend, K.; Zimmerman, S.; Kirner, S.; Schaup, J.; Schein, J.; Huismann, G. *Thermische Plasmen: Einfluss der Strommodulation und der Verwendeten Prozessgase auf den Lichtbogendrahtspritzprozess*; Band 9, Heft 2; Thermal Spray Bulletin; DVS Media GmbH: Dusseldorf, Germany, 2016; pp. 114–121.
25. Schatt, W.; Wieters, K.-P.; Kieback, P. *Pulvermetallurgie. Technologien und Werkstoffe: 2, Bearbeitete und Erweiterte Auflage*; Springer: Berlin/Heidelberg, Germany, 2007.